Figure 3. Differentiation capability of iPS-DP31 *in vitro* and *in vivo*. **(A-F)** Embryonic bodies were generated from iPS-DP31-4f-3 after floating in culture for 8 days (A), and subjected to adhesion culturing for 8 additional days (B). Cells that grew out from the EBs and were immunostained with second antibody (2nd Ab) only (C), βIII-tubulin (D, a marker of ectoderm), α-SMA (E, mesoderm marker) or AFP (F, endoderm marker) are shown. Nuclei were stained with Hoechst 33342 (C-F). Scale bar = 200 μm (A, B), and 100 μm (C-F). **(G-L)** To confirm the pluripotency of iPS-DP-4f-3 cells *in vivo*, we injected the cells into the testes of severe combined immunodeficiency (SCID) mice to generate teratomas. Nine weeks after injection, we observed tumor formation (G). Hematoxylin and eosin-stained teratoma sections show that the tumor contained various tissues, such as adipose tissue (H), nerve tissue (I), gut-like epithelial tissues (J), cartilage (K), and neural tube-like structures (L). AFP, alpha-fetoprotein; α-SMA, α-smooth muscle actin.

Table . List of Gifu collection of DPSC lines

Cell lines	Sex	Age	Stage	A-locus		B-locus		DR-locus	
DP1	M	14	CC	A24	A33	B61	B44	DR4	DR13
DP4	F	17	RF	A3	A24	B7	B13	DR1	DR7
DP6	F	16	RF	A2	A2	B35	B61	DR4	DR9
DP7	M	16	RF	A3	A24	B44	B52	DR9	DR15
DP10	F	15	CC	A24	A26	B13	B52	DR12	DR15
DP12	F	16	RF	A24	A31	B7	B56	DR1	DR14
DP13	F	15	RF	A31	A31	B61	B51	DR8	DR9
DP14	F	14	CC	A24	A31	B62	B52	DR9	DR15
DP15	F	15	CC	A2	A2	B75	B46	DR8	DR14
DP17	F	17	RF	A24	A26	B52	B54	DR9	DR15
DP20	F	18	RF	A26	A33	B44	B46	DR4	DR8
DP25	F	16	CC	A2	A24	B35	B51	DR4	DR8
DP26	F	14	CC	A2	A2	B71	B35	DR4	DR12
DP28*	M	14	CC	A2	A31	B35	B46	DR4	DR8
DP30	F	15	RF	A24	A31	B62	B52	DR9	DR15
DP31*	F	14	CC	A11	A31	B48	B55	DR9	DR11
DP32	F	20	RF	A24	A26	B61	B61	DR4	DR8
DP33	M	17	RF	A24	A26	B52	B54	DR14	DR15
DP35	F	18	RF	A33	A33	B44	B44	DR8	DR13
DP38	F	18	RF	A11	A31	B61	B51	DR4	DR14
DP39	F	13	CC	A11	A24	B62	B61	DR4	DR15
DP40	F	16	RF	A24	A26	B62	B52	DR14	DR15
DP41	F	17	RF	A24	A26	B54	B54	DR1	DR4
DP42	F	16	RF	A24	A24	B7	B51	DR1	DR8
DP44	F	14	CC	A24	A24	B60	B52	DR12	DR15
DP46	M	14	CC	A11	A24	B62	B51	DR4	DR14
DP48	M	15	CC	A24	A26	B62	B52	DR14	DR15
DP49*	F	12	CC	A24	A33	B7	B44	DR1	DR8
DP52	M	15	CC	A11	A26	B55	B67	DR8	DR16
DP53	F	15	CC	A24	A31	B7	B54	DR1	DR4
DP54*	M	19	RC	A2	A26	B61	B46	DR8	DR9
DP56	F	13	CC	A24	A24	B61	B52	DR9	DR15
DP57	F	18	RC	A24	A33	B44	B54	DR4	DR13
DP58	F	14	CC	A24	A26	B60	B61	DR11	DR9
DP59	F	16	RF	A24	A24	B7	B62	DR1	DR14
DP60	M	14	CC	A2	A24	B46	B52	DR8	DR15
DP62	F	16	RF	A24	A24	B48	B59	DR4	DR9
DP64	F	13	CC	A2	A2	B60	B46	DR8	DR14
DP65	F	18	RF	A24	A24	B61	B61	DR9	DR14
DP66	F	19	RF	A24	A24	B60	B51	DR8	DR11
DP68	F	13	CC	A24	A33	B62	B55	DR4	DR4
DP69	F	15	RF	A2	A24	B46	B52	DR9	DR15
DP72	F	16	RF	A2	A11	B60	B46	DR8	DR15
DP73	F	14	CC	A2	A31	B62	B60	DR8	DR9
DP74	F	16	RF	A24	A24	B52	B52	DR15	DR15
DP75*	M	24	RC	A2	A24	B62	B51	DR8	DR8
DP80	F	20	RC	A31	A33	B44	B51	DR9	DR13
DP81	M	16	RF	A24	A24	B7	B52	DR1	DR15
DP83	F	20	RC	A2	A26	B62	B60	DR8	DR15
DP86	M	17	RF	A24	A31	B51	B52	DR9	DR15
DP87*	F	20	RF	A24	A33	B51	B52	DR1403	DR15
DP92	F	14	CC	A2	A24	B71	B35	DR4	DR15
DP94	F	16	RF	A11	A11	B62	B62	DR4	DR4
DP95	M	16	RF	A24	A24	B35	B61	DR4	DR9
DP96	F	13	CC	A11	A24	B54	B58	DR8	DR13

DP97	M	16	RF	A24	A24	B52	B54	DR4	DR15
DP98	F	14	CC	A2	A24	B48	B54	DR4	DR4
DP99	F	19	RC	A24	A31	B62	B52	DR8	DR15
DP100	F	13	CC	A2	A33	B35	B51	DR4	DR4
DP101	M	16	RF	A33	A33	B44	B44	DR4	DR13
DP105	F	19	RF	A2	A24	B35	B61	DR4	DR4
DP106	F	13	CC	A24	A26	B62	B61	DR4	DR13
DP109	M	12	CC	A24	A24	B46	B54	DR4	DR15
DP111	F	17	RF	A33	A33	B44	B44	DR9	DR13
DP112	F	18	RC	A26	A33	B44	B55	DR13	DR15
DP113	F	17	RC	A11	A24	B51	B54	DR4	DR8
DP115	F	13	CC	A2	A24	B51	B60	DR9	DR14
DP128	F	13	CC	A24	A24	B62	B37	DR9	DR10
DP129	M	16	CC	A2	A11	B39	B67	DR4	DR15
DP134	F	17	CC	A31	A33	B44	B51	DR4	DR13
DP135	M	17	CC	A33	A33	B62	B44	DR13	DR14
DP136	F	15	CC	A11	A24	B52	B54	DR8	DR15
DP138	F	17	RF	A2	A24	B61	B46	DR8	DR12
DP140	M	19	RC	A31	A33	B62	B39	DR9	DR15
DP141	F	22	RC	A2	A24	B60	B52	DR15	DR15
DP142	M	21	RC	A2	A33	B62	B44	DR9	DR15
DP143	F	19	RF	A24	A24	B54	B52	DR14	DR15
DP144	F	15	CC	A2	A33	B44	B44	DR13	DR13
DP147	F	14	RF	A24	A24	B51	B52	DR4	DR15
DP153	M	18	RF	A2	A2	B62	B55	DR4	DR4
DP154	F	21	RC	A2	A24	B62	B52	DR15	DR15
DP157	F	20	RC	A2	A33	B7	B44	DR1	DR4
DP158	M	19	RC	A24	A33	B51	B52	DR9	DR15
DP159	M	23	RC	A2	A24	B75	B46	DR8	DR15
DP160	F	13	CC	A2	A24	B61	B54	DR4	DR13
DP163	F	13	CC	A24	A26	B61	B46	DR4	DR9
DP164	F	24	RC	A2	A24	B39	B60	DR12	DR12
DP165	F	24	RC	A24	A24	B7	B62	DR1	DR9
DP166	F	23	RC	A24	A33	B60	B44	DR4	DR16
DP167	F	18	RF	A24	A24	B60	B52	DR4	DR15
DP169	M	16	RF	A2	A26	B60	B51	DR8	DR15
DP170	F	18	RF	A2	A24	B51	B54	DR4	DR9
DP172	M	17	RF	A2	A24	B60	B52	DR4	DR15
DP173	F	14	RF	A1	A33	B37	B44	DR10	DR14
DP174	F	15	CC	A2	A24	B44	B48	DR4	DR13
DP175	F	20	RC	A2	A33	B7	B44	DR1	DR4
DP176	M	17	CC	A24	A24	B62	B61	DR4	DR9
DP177	F	13	CC	A24	A33	B60	B44	DR13	DR14
DP178	F	13	CC	A24	A24	B61	B52	DR12	DR15
DP179	F	19	RF	A2	A24	B39	B51	DR8	DR15
DP181	M	20	RC	A2	A26	B46	B48	DR8	DR9
DP182	M	16	RF	A24	A31	B27	B59	DR13	DR15
DP184	F	52	RC	A24	A33	B44	B52	DR13	DR15
DP185	M	62	RC	A2	A24	B39	B51	DR15	DR15
DP186	F	17	RF	A2	A11	B54	B54	DR4	DR14
DP187	F	22	RC	A2	A2	B13	B46	DR8	DR12
DP193	M	60	RC	A24	A26	B39	B52	DR8	DR15

* DPSC lines used for induction of iPS cells in this study. Stage indicates the developmental stages of tooth isolated from patients to establish DPSC lines. Abbreviation: CC, crown-completed stage; RF, root-forming stage; RC, root-completed stage.

Tamaoki *et al.* Figure 1

A

Cell lines	DP28	DP31	DP49	DP54	DP75	DP87
Sex	Male	Female	Female	Male	Male	Female
Age	14	14	12	19	24	20
Stages	CC	CC	CC	RC	RC	RF

B

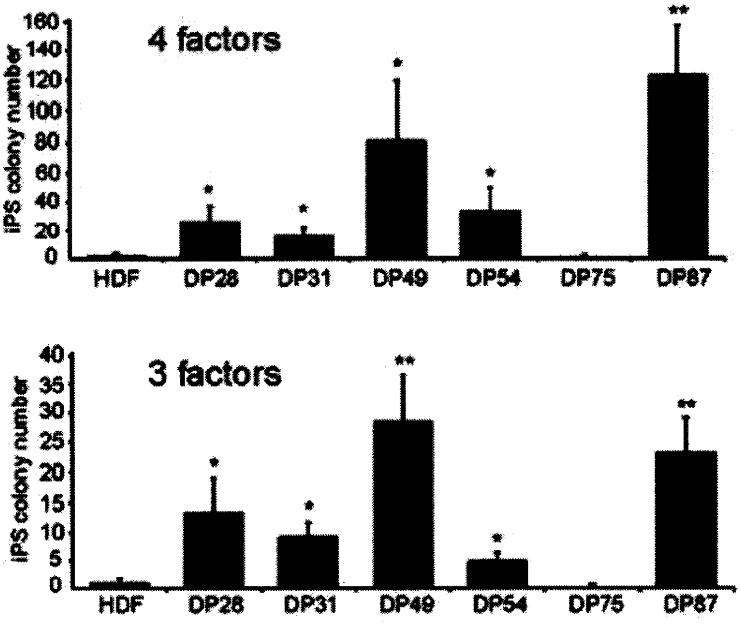

C

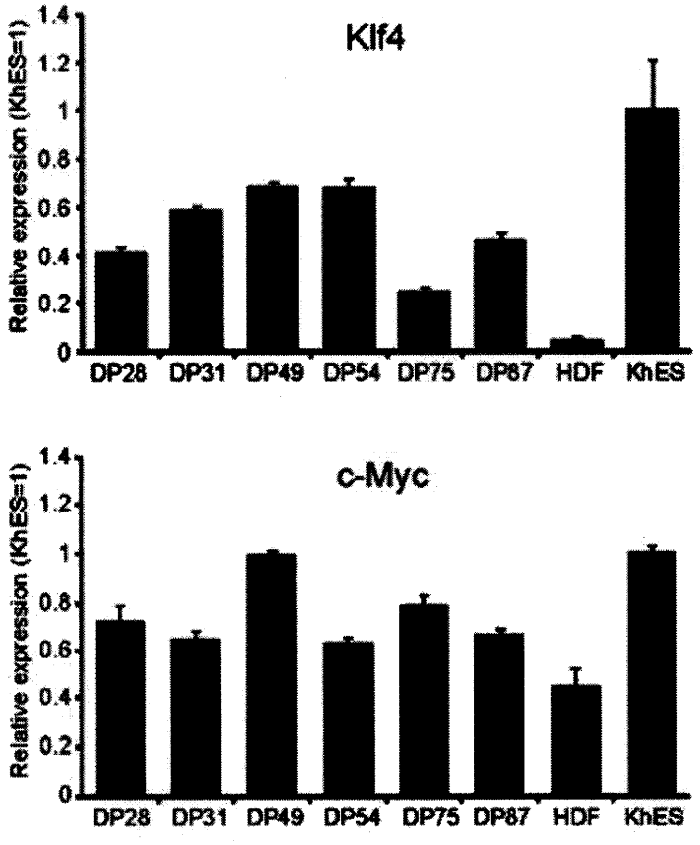

Tamaoki *et al.* Figure 2

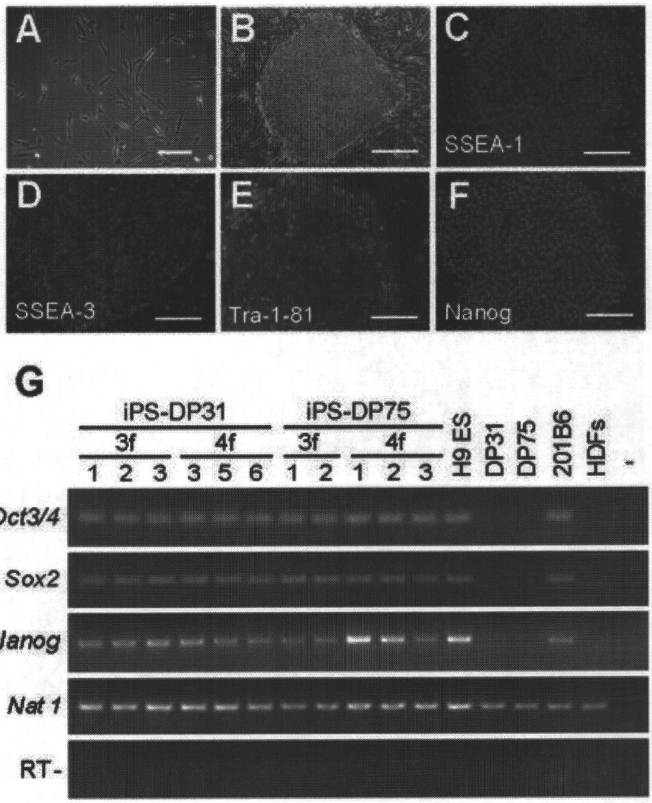

Tamaoki *et al.* Figure 3

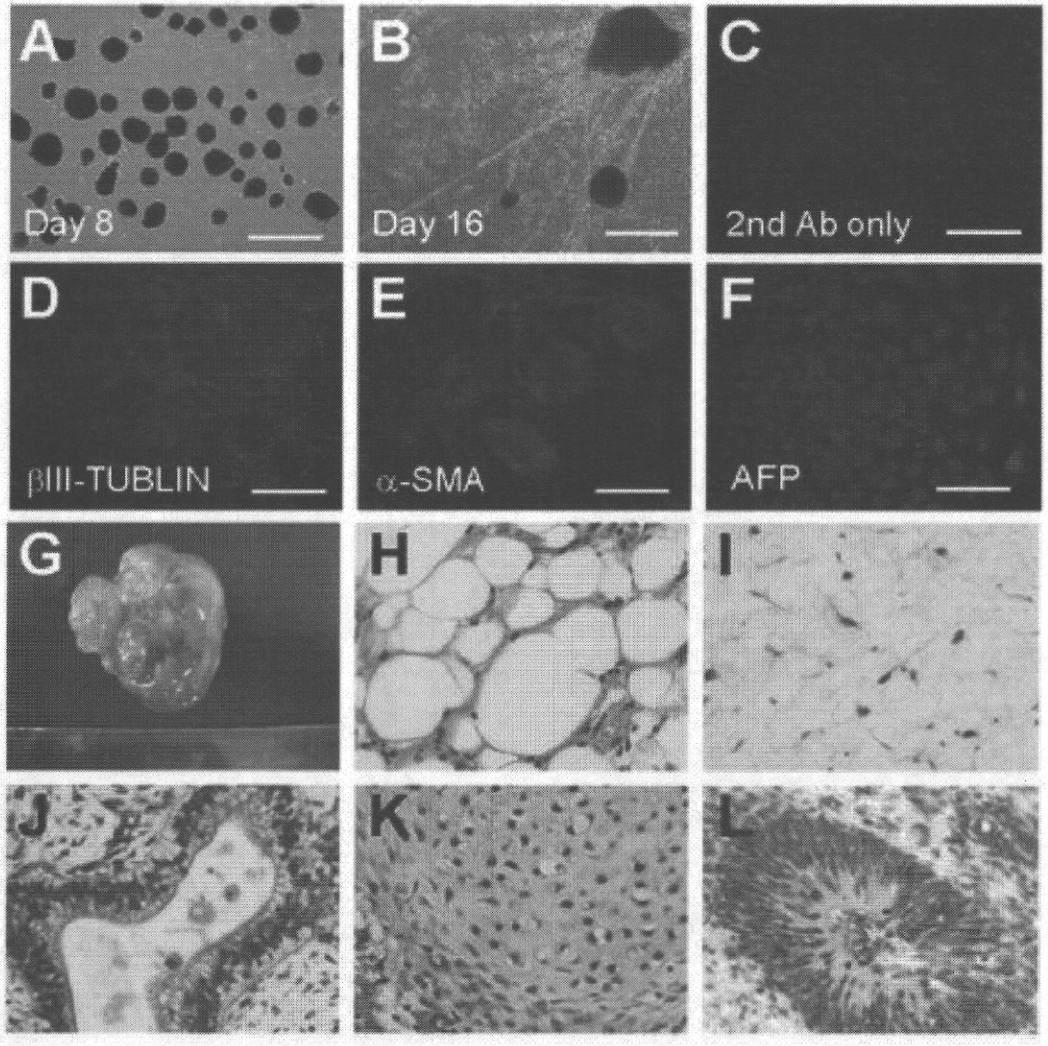

Functionally distinct melanocyte populations revealed by reconstitution of hair follicles in mice

Hitomi Aoki[1], Akira Hara[2], Tsutomu Motohashi[1], Masatake Osawa[3] and Takahiro Kunisada[1]

1 Department of Tissue and Organ Development, Regeneration, and Advanced Medical Science, Gifu University Graduate School of Medicine, Yanagido, Gifu, Japan **2** Department of Tumor Pathology, Regeneration, and Advanced Medical Science, Gifu University Graduate School of Medicine, Yanagido, Gifu, Japan
3 Department of Dermatology, Cutaneous Biology Research Center, Massachusetts General Hospital, Harvard Medical School, MA, USA

CORRESPONDENCE T. Kunisada, e-mail: tkunisad@gifu-u.ac.jp

KEYWORDS melanocytes/hair reconstitution assay/cell lineage/kit/Endothelin3

PUBLICATION DATA Received 30 August 2010, revised and accepted for publication 28 October 2010, published online 4 November 2010

doi: 10.1111/j.1755-148X.2010.00801.x

Summary

Hair follicle reconstitution analysis was used to test the contribution of melanocytes or their precursors to regenerated hair follicles. In this study, we first confirmed the process of chimeric hair follicle regeneration by both hair keratinocytes and follicular melanocytes. Then, as first suggested from the differential growth requirements of epidermal skin melanocytes and non-cutaneous or dermal melanocytes, we confirmed the inability of the latter to be involved as follicular melanocytes to regenerate hair follicles during the hair reconstitution assay. This clear functional discrimination between non-cutaneous or dermal melanocytes and epidermal melanocytes suggests the presence of two different melanocyte cell lineages, a finding that might be important in the pathogenesis of melanocyte-related diseases and melanomas.

Introduction

Melanocytes develop from the pluripotent neural crest (NC), which also gives rise to a number of other cell types; including neurons and glial cells of the peripheral nervous system as well as bone and cartilage cells of the head skeleton. The immature form of melanocytes, called the melanoblast, migrates along characteristic pathways to various destinations, such as the dermis and epidermis, the inner ear, and the choroid layer of the eye (for reviews see Hall, 2009; Le Douarin and Kalcheim, 1999). Unlike other NC cells, melanocyte precursors can differentiate from the NC irrespective of the region along the rostro-caudal axis. They migrate from the NC region and start to express the receptor tyrosine kinase Kit (in mice) in the migration staging area and then move toward the entrance of the migration route (dorsolateral pathway) prepatterned with Kitl (Kit ligand)/SCF (stem cell factor)-expressing cells (for example, the epithelial dermatome and overlying epidermis; Kelsh et al., 2009; Wehrle-Haller and Weston, 1997). These melanocyte precursors target the skin (dermis and epidermis) of the whole body. In mammals, skin melanocytes have been proposed to be classified as classical melanocytes and are involved in skin and hair pigmentation. Non-classical melanocytes are localized in the eye, inner ear, meninges, bone, and heart, having taken the dorso-ventral route rather than the dorsolateral one used by classical melanocytes (Yajima and Larue, 2008). According to some reports, to migrate correctly, the interaction of melanocytes (melanophores) and their surrounding microenvironment must be coordinated, or at least act simultaneously, to express

Significance

By using the hair follicle reconstitution assay, we show that dermal-type melanocytes were not integrated into the hair follicles and the hairs reconstituted with dermal-type melanocytes were not pigmented. Our results suggest the possible early separation of melanocyte sub-lineages that migrate either into the epidermis or into the dermis. These findings may assist in the future design of treatment for diseases such as melanocytosis, vitiligo, and melanomas.

Kit and Kitl (Alexeev and Yoon, 2006; Jeon et al., 2009; Randall et al., 2008).

The interaction between melanocytes and their surrounding tissues is typically manifested in transgenic mice in which Kitl expression in the skin is induced by the human cytokeratin 14 promoter. In this transgenic mouse, *hk14-Kitl*, melanocytes extend their niche to the interfollicular epidermal skin (Kunisada et al., 1998). Interestingly, in transgenic mice expressing Endothelin3 (*hk14-ET3*) or HGF (*hk14-HGF*), melanocytes are distributed mostly in the dermal skin, not the epidermal skin (Kunisada et al., 2000; Yamazaki et al., 2005), indicating that environmental factors may affect melanocyte distribution in the body. In *hk14-Kitl; hk14-ET3* and *hk14-Kitl; hk14-HGF* double transgenic mice, melanocytes are distributed in both dermal and epidermal skin, as if the characteristic expression of melanocytes in each single transgenic mouse had been superimposed. This finding suggests a rather independent maintenance of dermal and epidermal melanocyte populations (Aoki et al., 2009). In fact, comparisons of growth factor dependencies of melanocytes on KITL, ET3, HGF or other signals revealed that dermal or non-cutaneous melanocytes are not as sensitive to KIT signaling as the epidermal melanocytes, depending instead more on ET3 and HGF signaling (Aoki et al., 2009). Based on these findings, we have proposed the existence of two major melanocyte populations: KIT-sensitive cutaneous melanocytes in the epidermis and weakly KIT-sensitive non-cutaneous and dermal melanocytes.

However, there is a simpler argument that these two populations are separated by a barrier such as the basement membrane and can be functionally interchangeable. To examine this, we introduced the phenotype of double transgenic mice expressing dominant-negative KitV620A and ET3. These animals have a heavily pigmented dermal skin and mostly unpigmented epidermis and hair follicles. During their lifetime, the stability of the phenotype suggested to us the incompatible nature of these two melanocyte populations (Aoki et al., 2009).

To test our hypothesis, we took advantage of the hair follicle reconstitution assay (Lichti et al., 1993). In this assay, dermal and epidermal skin cells are completely dissociated into single cells, simply mixed, and start to regenerate complete skin tissues including hair follicles in vivo. If the dermal melanocytes or their precursors are contained in a dissociated skin sample they will at least have a chance to associate directly with developing hair follicles in this assay. We confirmed melanocyte reconstitution in the hair follicle using this hair reconstitution assay and then tested the potential of dermal melanocytes and non-cutaneous melanocytes outside of the epidermal skin to function as follicular melanocytes. Our results revealed a functional difference between dermal or other non-cutaneous melanocytes and epidermal melanocytes, which behaved almost like different cell lineages.

Results

The coat color of reconstituted skin: interaction between melanocytes and hair follicles

For manipulation of follicular melanocytes, follicular tissues containing melanocytes are transplanted to embryonic or neonatal mouse skin (Nishimura et al., 2002; Oshima et al., 2001). However, direct transfer of melanocytes to the hair follicles for hair pigmentation is not generally feasible. Although we successfully transferred dissociated melanocytes to uveal tissues (Aoki et al., 2008a,b), transplantation of purified melanocytes or a piece of tissue containing melanocytes to hair follicles does not restore hair pigmentation (unpublished observation by HA and TK). To examine the potential of individual melanocytes to induce hair pigmentation, we used the in vivo hair follicle reconstitution method described previously (Kamimura et al., 1997; Lichti et al., 1993). Freshly prepared cell suspensions composed of epidermal cells (primary keratinocytes) and dermal cells from C57BL/6, ICR, and C3H mice were grafted onto the back skin of nude mice. The resultant hairs in the regenerated skin were colored black, white, and agouti, respectively (Figure 1A–C). To confirm that the regenerated skin and hair follicles had a normal hair cycle, we plucked the first regenerated hairs. About 1 month later, second hairs of the same color as the first were formed (Supporting information Figure S1A–I). The mice in the hair reconstitution assay of C57BL/6, ICR, and C3H mice all developed four major hair types [zigzag, guard (monotrich), auchene, and awl] (Supporting information Figure S2F–H) and the regenerated skin had the normal morphology, including size and shape of the hair follicles (Supporting information Figure S2K–M), although the angle of the hair follicles to the skin surface and the depth of the lower part of the follicles were not constant, unlike in normal skin. Importantly, the normal regeneration of the hair follicles including pigmented hairs after plucking the hair indicates that the stem cell systems of hair follicles and melanocytes had functionally regenerated.

When the cells prepared from the C57BL/6 and ICR mice were mixed 1:1 and then grafted onto the back skin of nude mice, the resultant hair follicles showed the agouti color (Figure 1D). Individual cells from C57BL/6 and ICR mice generated black and white hairs, respectively (Figure 1E). As shown previously by dermal–epidermal recombination of mouse skin, hair follicles generated from the mixture of the skin cells from C57BL/6 mice with the *a/a C/C* coat color genotype and ICR ones with *A/? c/c* grew agouti-colored hairs (Mayer and Fishbane, 1972). The agouti signal proteins encoded by the agouti (*A*) locus of the albino (*c*) ICR mouse-derived dermal papilla cells direct the pheomelanin synthesis of follicular non-albino (*C*) melanocytes derived from C57BL/6 mice (Jackson, 1993; Ollmann et al., 1997). The

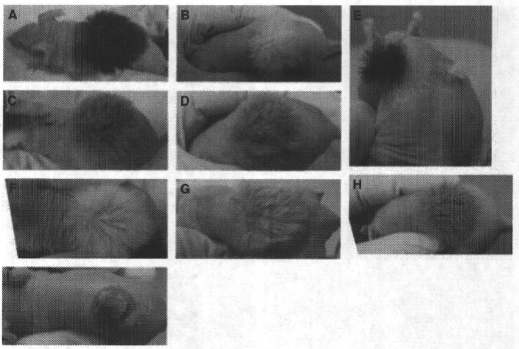

Figure 1. Reconstituted hairs generated in the hair reconstitution assay. (A–E) Reconstituted hairs from the skin of newborn mice in the hair reconstitution assay. Epidermal cells and dermal cells prepared from the skin of C57BL/6 (A), ICR (B), C3H (C), C57BL/6 and ICR, 1:1 (D), and individual C57BL/6 (left area) and ICR (right area, E) mice were used. (F–H) Reconstituted hairs from various mixtures of the C57BL/6 and ICR skin cells: 1:9 (F), 1:1 (G), and 3:7 (H). (I) Reconstituted hairs from the mixture of the C57BL/6 skin and *Kit V620A Tg4* transgenic skin.

regenerated hair follicles also showed normal hair cycle progression, although the second regenerated hairs were slightly lighter in color (Supporting information Figure S1J–L). When the ratio of cells prepared from the C57BL/6 and ICR mice was varied as 1:9, 5:5, and 7:3, the resultant agouti hair colors changed (as shown in Figure 1F–H). Based on these experiments, melanocytes and dermal papilla cells derived from the skin of different mice must have formed individually chimeric hair follicles.

We previously reported a mouse model of human piebaldism comprising the Val620Ala mutation in the *Kit* gene; this model shows various coat-pigmentation patterns among the transgenic lines generated (Tosaki et al., 2006). In *KitV620ATg-4*, which is a relatively less pigmented line, we sometimes found almost completely white individuals (Supporting information Figure S3A, B). When cells were prepared from the mixture of C57BL/6 mouse skin cells and completely white *KitV620ATg-4* skin cell and the cells grafted onto the back skin of nude mice, the resultant hairs showed the mix of the black (pigmented) and the white (non-pigmented) hairs (Figure 1I) but not the agouti hairs observed in the ICR and C57BL/6 combination. Regenerated hairs after plucking were again a mixture of the black and white hairs (Supporting information Figure S1M). This finding confirms that the genotypes of the hair follicle components are important for melanocyte pigmentation.

Hair follicles regenerated from the mixture of the primary keratinocytes from C57BL/6 epidermal skin and dermal cells from ICR dermal skin contained mostly white hair (Supporting information Figure S2A). Hair follicles regenerated from the mixture of the C57BL/6 dermal skin and ICR epidermal cells formed black hair (Supporting information Figure S2B) but not agouti. The results may simply indicate that the dermal part of the separated skin was the main contributor of the regenerated hair follicles including melanocytes. Mice in the hair reconstitution assay of C57BL/6, ICR, and C3H mice developed four major hair types (Supporting information Figure S2I,J) and the regenerated skin had a normal morphology including size and shape of the hair follicles (Supporting information Figure 2N,O), although the angle of the hair follicles to the skin surface and the depth of the lower part of the follicles were not constant, unlike in normal skin. In our experiment, neonatal skins were treated with 0.25% trypsin/EDTA and the epidermal sheets were separated by gentle stirring. Under microscopic observation, hair follicles including epidermal components were shown to be caught in the dermal compartments (Supporting information Figure 2C–E) along with follicular melanocytes. Reconstitution with only the epidermal skin cells produced mostly hairless skin, whereas small numbers of hairs were observed using the dermal skin cells only (data not shown), suggesting that some portion of epidermal cells were retained in the dermal skin part, at least with our method, as shown in Supporting information Figure S2C–E.

Chimeric status of reconstituted hair follicles including melanocytes

To examine more directly whether hair follicles generated by the reconstitution assay were chimeras of individual skins, we used the combination of *DCT-Cre/DCT-Cre; CAG-GAT-EGFP/CAG-GAT-EGFP* transgenic mice and wild-type mice. After reconstitution by an equal number of these two types of skin cells, the hair follicles formed showed various ratios of GFP-positive and GFP-negative cells (Figure 2A,B). With the combination of *CAG-EGFP* epidermal skin and wild-type dermis, epidermal components in some hair follicles were GFP-positive, but most of the hair follicles were GFP-negative (Figure 2C,D), as suggested in Supporting

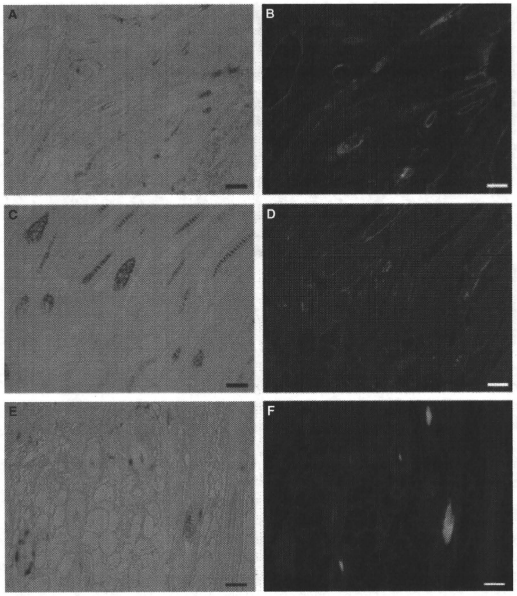

Figure 2. Histology of the reconstituted hairs generated in the hair reconstitution assay. (A and B) Reconstituted hairs from a mixture of *DCT-Cre/Dct-Cre; CAG-GAT-EGFP/CAG-GAT-EGFP* mouse line and wild-type mouse line cells in the hair reconstitution assay. (C,D) Reconstituted hairs from a mixture of cells from newborn *CAG-EGFP* mouse line epidermis and wild-type mouse line dermis in the hair reconstitution assay. (E,F) Reconstituted hairs from a mixture of skin cells from newborn *DCT-Venus* mouse line and *DCT-LacZ* mouse line in the hair reconstitution assay. (A,C,E) Phase-contrast images. (B,D,F) GFP fluorescent images. Scale bars: 50 μm.

information Figure S2. These results indicate that the regenerated hair follicles were truly chimeric; a single regenerated hair follicle originated from multiple founder cells.

To examine whether these chimera hair follicles generated by the reconstitution assay were also chimeric with respect to melanocytes, we used the combination of *DCT-Venus* and *DCT-LacZ* transgenic mice for the hair follicle reconstitution. Venus is an improved variant of YFP (Nagai et al., 2002). Both transgenic mouse strains express marker proteins under the melanocyte-specific *DCT* gene promoter sequence. As shown in Figure 2(E,F), Venus-positive melanocytes and LacZ-positive melanocytes from different mouse skins were found in single hair follicles, indicating that the melanocyte showed the multiple melanocyte lineage progenitors in single reconstituted hair follicles.

Dermally restricted re-distribution in the reconstituted skin of melanocytes derived from *hk14-ET3* mice: no integration of dermal melanocytes into the epidermal follicular structures

With the above results we now had the experimental basis to examine whether dermal melanocytes have the potential to contribute to hair pigmentation in the hair follicle reconstitution assay. *hk14-ET3* transgenic mice, the dermal melanocytosis model we developed, contain a large number of melanocytes in their dermal skin. To remove epidermal or follicular melanocytes present in the *kh14-ET3* transgenic mice (Figure S3C,D), we used *hk14-ET3/+; Kit V620A Tg4/?* double transgenic mice (Figure 3A and Supporting information Figure S3E,F) in which the dominant-negative Kit receptor transgene selectively eliminates follicular epidermal melanocytes (Aoki et al., 2009). The double transgenic mice rarely have epidermal melanocytes in their trunk, as shown by the white coat color, but dermal melanocytes are maintained throughout their life.

In the hair follicle reconstitution assay using the skin from *hk14-ET3/+; Kit V620A Tg4/?* mice, these animals regenerated skin with black-pigmented dermis and non-pigmented epidermis with white hair (Figure 3B,C). In contrast, in the hair reconstitution assay using the skin from *Kit V620A Tg4/?* mice as a control, these animals regenerated skin with non-pigmented dermis and epidermis with white hair (Figure 3D,E). Morphological analysis of the regenerated *hk14-ET3/+; Kit V620A Tg4/+* skin confirmed that there were no melanocytes

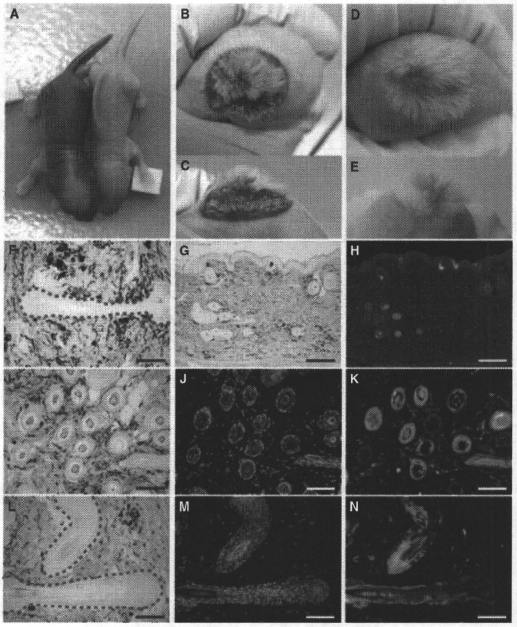

Figure 3. Reconstituted hairs from newborn mouse skin cells of the black-pigmented dermis with white hair mouse line. (A) A mouse pup with black-pigmented dermis and white hair (*hk14-ET3/+; Kit V620A Tg4/+*, left pup) derived from a cross between an *hk14-ET3/+* mouse and *Kit V620A Tg4/+* mouse. Photographs were taken at P2. The *Kit V620A Tg4/+* mouse is shown at the right side. (B,C) Reconstituted hairs from skin cells of *hk14-ET3/+; Kit V620A Tg4/?* newborn mouse in the hair reconstitution assay. (D,E) Reconstituted hairs from *Kit V620A Tg4/?* mouse line in the hair reconstitution assay. (F) Histology of the reconstituted hairs from *hk14-ET3/+; Kit V620A Tg4/+* newborn skin cells. (G–N) Histology of the reconstituted hairs from *hk14-ET3/+; Kit V620A Tg4/Tg4; CAG-EGFP/+* and *Kit V620A Tg4/Tg4* skins. (F,G,I,L) Phase-contrast images. (J,M) Nuclear counterstaining using Hoechst stain. (H,K,N) GFP fluorescent images. The dotted lines in F and I show the boundary of hair follicles. Scale bars: 50 μm.

in the epidermis or in the hair follicles of these mice, in spite of the abundant expansion of the melanocytes in the dermis (Figure 3F). Based on the experiments in the previous section, we can safely expect that the regenerated hair follicles were potentially chimeras of the melanocytes from every hair follicle used for the assay. To further exclude the possibility that each of the regenerated hair follicles originated only from a single hair follicle of *hk14-ET3/+; Kit V620A Tg4/+* mice, we reconstituted the mixture of the cells from *hk14-ET3/+; Kit V620A Tg4/Tg4; CAG-EGFP/+* triple transgenic mice and *Kit V620A Tg4/Tg4* mice. The results shown in Figure 3(G,H) clearly indicate that the regenerated hair follicles were chimeras of GFP-positive and GFP-negative cells derived from each transgenic mouse. Also, by observing serial sections from the same specimens, we again confirmed that no melanocytes had been integrated into these regenerated chimeric hair follicles (Figure 3I–N and data not shown).

Pigmentation in the dermis remained unchanged for more than 6 months, indicating that the dermal melanocytes had probably been regenerated, including their stem cells. This notion was supported by the fact that adult *hk14-ET3/+; Kit V620A Tg4/+; DCT-LacZ/+* dermal skin contained unpigmented LacZ-positive cells, melanocyte precursors, as did *hk14-ET3/+; DCT-LacZ/+* skin (Supporting information Figure S4A–D).

Reconstituted hair follicles formed by *hk14-ET3/+; Kit V620A Tg4/+* skin cells are capable of accepting follicular melanocytes

hk14-ET3/+; Kit V620A Tg4/+ mice rarely have pigmented hairs; however, the existence of small patches of pigmented hairs is evidence that the hair follicles are able to receive melanocytes (Figure 4A). To fully exclude the possibility that the regenerated *hk14-ET3/+; Kit V620A Tg4/+* hair follicles cannot integrate melanocytes, we mixed the skins from *hk14-ET3/+; Kit V620A Tg4/+* mice with those from partially pigmented (about 10–20% of the total area) *Kit V620A Tg4/?* mice. The reconstituted skin contained black-pigmented dermis with pigmented hair follicles (Figure 4B,E,H). Skin cells prepared from *hk14-ET3/+; Kit V620A Tg4/+* mice or the mixture of

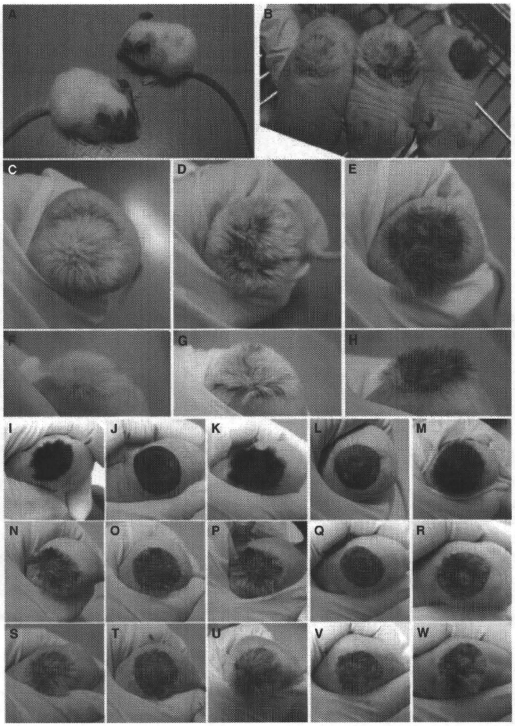

Figure 4. Reconstituted hairs generated from the combination of skin cells from the black-pigmented dermis with white hair mouse line and skin cells from the black hair area from a *Kit V620A Tg4/Kit V620A Tg4* mouse. (A) A mouse pup with black-pigmented dermis and white hair derived from a cross between a *hk14-ET3/+* mouse and a *Kit V620A Tg4/+* mouse (right side). Photographs were taken at P16. The *Kit V620A Tg4/Kit V620A Tg4* mouse is shown at the left side. (B–H) Reconstituted hairs from skin cells of an *hk14-ET3/+* and a *Kit V620A Tg4/+* newborn mouse combined or not with those of a *Kit V620A Tg4/Kit V620A Tg4* newborn in the hair reconstitution assay. The mouse on the left in B and the mouse in C and F are the same mouse grafted with cells from *hk14-ET3/+; Kit V620A Tg4/+* newborn mouse skin and completely white *Kit V620A Tg4/Kit V620A Tg4* mouse newborn skin without pigmented areas. The mouse in the middle in B and the mouse in D and G are the same mouse grafted with cells from *hk14-ET3/+; Kit V620A Tg4/+* newborn mouse skin. The mouse on the right in B and the mouse in E and H are the same mouse grafted with cells from *hk14-ET3/+; Kit V620A Tg4/+* newborn mouse skin and partially pigmented *Kit V620A Tg4/Kit V620A Tg4* newborn mouse skin (pigmented areas comprised about 10–20% of the total area). (I–W) Reconstituted hairs from *hk14-ET3/+* newborn mouse skin and from the mixture of the cells from *hk14-ET3/+; Kit V620A Tg4/+* newborn mouse skin and partially pigmented *Kit V620A Tg4/Kit V620A Tg4* newborn mouse skin (pigmented areas comprised about 10–20% of the total area) in the hair reconstitution assay. (I–M) *hk14-ET3/+*, (N–W) *hk14-ET3/+; Kit V620A Tg4/+* and partially pigmented *Kit V620A Tg4/Kit V620A Tg4*. (I,N,S) The first hairs after the hair reconstitution assay. (J,O,T) Skins after plucking the first reconstituted hairs. (K,P,U) Secondary regenerated hairs. (L,Q,V) Skins after plucking the secondary regenerated hairs. (M,R,W) The third regenerated hairs.

skin cells from *hk14-ET3/+; Kit V620A Tg4/+* mice and unpigmented *Kit V620A Tg4/?* mice both reconstituted the black-pigmented dermis with white hairs (Figure 4C,D,F,G). These results indicate that the regenerated hair follicles from *hk14-ET3/+; Kit V620A Tg4/+* mice had the potential to support melanocytes whenever the potent follicular epidermal-type melanocytes were available.

To confirm whether these pigmented hair follicles that were regenerated from the pigmented skin regions from *KitV620ATg4/?* mouse have the melanocyte stem cells that self-renew in the next hair cycle (Figure 4I,N,S), we plucked the first regenerated hairs (Figure 4J,O,T). About 1 month later, the secondary hairs showed the same color as the first regenerated hairs (Figure 4K,P,U). We again plucked these regenerated hairs (Figure 4L,Q,V). Even after the third cycle, the hairs still grew back as black ones (Figure 4M,R,W). These results indicated that the hair follicles of the regenerated skin from *hk14-ET3/+; Kit V620A Tg4/+* mice were capable of supporting melanocyte development during the regeneration process, including the maintenance of stem cells.

Dermally restricted re-distribution of non-cutaneous melanocytes in the reconstituted skin

Dermal melanocytes are known to be gradually lost after birth (Hirobe, 1984), and therefore the dermal melanocytes generated in the *hk14-ET3* transgenic mouse skin might have very different physiological properties compared to their normal counterparts. As a substitute for the normal dermal melanocytes, we used non-cutaneous melanocytes from harderian gland and choroid in the hair reconstitution assay. Melanocytes in these tissues have growth factor requirements different from those of epidermal follicular melanocytes (Aoki et al., 2009). To examine the potential of melanocytes from harderian gland or choroid, we combined *Kit V620A Tg4/Tg4; DCT-LacZ/+* mouse skin cells with harderian gland cells or choroid cells including melanocytes or their precursors. The reconstituted hair follicles had mostly white hairs, pigmented hairs were rarely found (Figure 5A–D), indicating that melanocytes in the harderian gland or choroids were not integrated into the regenerated hair follicles. The melanocytes in these rarely found pigmented hairs were LacZ-positive (Figure 5E,F), derived from *Kit V620A Tg4/Tg4; DCT-LacZ/+* mouse skin. We also observed LacZ-positive, round-shaped cells, which must have been derived from *Kit*

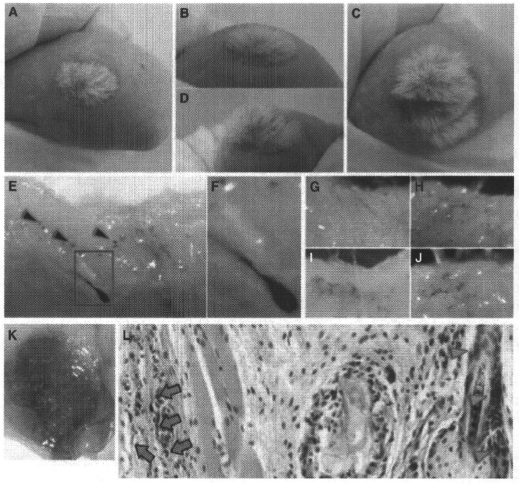

Figure 5. Reconstituted hairs with non-cutaneous melanocytes used in the hair reconstitution assay. (A,B) Reconstituted hairs from *Kit V620A Tg4/Kit V620A Tg4; DCT-LacZ/+* newborn mouse skin cells combined with adult mice choroid cells including melanocytes. (C,D) Regenerated hairs from *Kit V620A Tg4/Kit V620A Tg4; DCT-LacZ/+* newborn mouse skin cells combined with adult mouse harderian gland cells including melanocytes. (E,F) LacZ staining of the dissection of the reconstituted skin generated from *Kit V620A Tg4/Kit V620A Tg4; DCT-LacZ/+* newborn mouse skin cells combined with adult mouse choroid cells including melanocytes. Red square regions in E were enlarged in F. Arrowheads in E indicate the LacZ-positive, round-shaped, non- dendritic cells outside the pigmented hairs. (G–J) LacZ staining of the dissection of the reconstituted skin generated from *Kit V620A Tg4/Kit V620A Tg4; DCT-LacZ/+* newborn mouse skin combined with adult mouse harderian gland cells including melanocytes. (K,L) Patch assays including non-cutaneous melanocytes. (K) A patch assay using a mixture of non-cutaneous choroid tissues including melanocytes from P0 wild type and skin cells from *Kit V620A Tg4/Tg4; DCT-LacZ/+* mice. (L) Histological analysis of K. Arrowheads indicate the DCT-LacZ-positive follicular melanocytes from Kit *V620A Tg4/Tg4; DCT-LacZ/+* mouse and arrows indicate non-cutaneous melanocytes derived from choroid.

V620A Tg4/Tg4; DCT-LacZ/+ mouse skin outside of the reconstituted hair follicles (Figure 5E, arrowheads). In the dermis of the reconstituted skin, we often found LacZ-negative pigmented melanocytes, likely originating from harderian gland or choroids (Figure 5G–J).

To strengthen our results quantitatively, we utilized the patch assay, which is another method for hair follicle reconstitution (Zheng et al., 2005). This method introduces skin-derived cells by subcutaneous injection; after injection, the regenerated hair follicles were found in the dermally formed dermoid cysts. We used the dissociated skin cells from *Kit V620A Tg4/Tg4; DCT-LacZ/+* mice and wild-type mice choroids as non-epidermal melanocytes sources for the patch assay (Figure 5K). In this case, we also found many LacZ-negative melanocytes, but only outside of the regenerated hair follicles (Figure 5L). In conclusion, non-cutaneous melanocytes, such as melanocytes from the harderian gland or choroid, were maintained in the dermal region, but they did not integrate and remain as melanocyte stem cells in the regenerated hair follicles.

Discussion

We previously reported that two distinct types of mouse melanocyte, namely, dermal or non-cutaneous melanocytes and epidermal melanocytes, can be distinguished based on their different signaling requirements. This was plainly observed in the black-pigmented dermis with white hair in *Kit V620A; hk14-ET3* double transgenic mice (Aoki et al., 2009). In the present study, we focused on the functional difference between these melanocyte cell types by asking whether dermal or non-cutaneous melanocytes can be integrated into hair follicles to provide the melanin pigment granules. Using the hair follicle reconstitution assay, we showed that the dermal-type melanocytes never became integrated into the hair follicles and therefore that the hairs reconstituted with dermal-type melanocytes were unpigmented.

Skin is mainly composed of two types of cells: one is the epidermal keratinocyte of ectodermal origin, and the other is the fibroblast, likely of mesodermal origin. In contrast to the classical histogenetic aggregation of dissociated cells (Moscona, 1961), the reconstitution assay described here took longer to generate skin tissue. Skin structures including hair follicles were established within 72 h by the histogenetic aggregation reported by Monroy and Moscona (1979), but more than a week was necessary before a skin-like thin structure under the scab could be observed in the hair follicle reconstitution assay, indicating that this assay is recapitulating the developmental process of the skin, not simple reorganizing tissues after aggregation. It is known that histogenetic aggregation of dissociated cells is only possible in the case of embryonic tissues or neonate tissues (Monroy and Moscona, 1979); in contrast, the hair follicle reconstitution assay is applicable for adult skin cells. This also implies that the hair follicle reconstitution assay used here truly represents a regenerative process starting from restricted stem cell populations. In fact, mosaic analysis using ES cell injection chimera revealed that the hair bulb region was composed of multiple but four or fewer progenitors (Kopan et al., 2002).

We used transgenic mice exogenously expressing ET3 as the experimental source of dermal-type melanocytes. Since transgenic ET3 is driven by the cytokeratin 14 regulatory sequence and the regeneration process mimics embryogenic skin development, as discussed above, the dermal melanocytes of ET3 transgenic mice lack ET3 signaling for a certain period of time until the regenerating keratinocytes start to express ET3. However, because the cytokeratin 14 promoter drives transcription in the mouse embryo as early as embryonic day 9.5, and a large number of keratinocytes were added at the start of the reconstitution assay, it is likely that dermal melanocyte precursors or stem cells survived during the early phase of the assay. Using non-cutaneous melanocytes such as choroid and harderian gland melanocytes, we further confirmed that these non-cutaneous melanocytes were also scarcely included in the regenerated hair follicles.

It is widely accepted that all melanocytes are derived from the neural crest cell lineage, even after the recent finding that some melanocytes originate from Schwann cell precursors, which are also descendants of neural crest cells (Adameyko et al., 2009). It is therefore surprising that dermal melanocytes are incompatible for integration into hair follicles, also considering that even cultured human epidermal melanocytes are capable of regenerating pigmented hairs in the hair follicle reconstitution assay (Tsunenaga and Ideta, 2002 and M. Tsunenaga and R. Ideta, personal communication). Obviously, most of the melanocytes regenerated in our reconstitution assay had developed from non-pigmented precursors or stem cells present in each cell source (Figure S4). During early embryogenesis, melanocyte precursors departing from the NC region express Kit in the migration staging area and move toward the entrance of the migration route (dorsolateral pathway) prepatterned with KITL-expressing cells (for example, the epithelial dermatome and overlying epidermis) (Kelsh et al., 2009; Wehrle-Haller and Weston, 1997). Dorsolaterally moving melanoblasts simultaneously migrate from the dermis to the epidermis (Yoshida et al., 1996a), perhaps indicating that molecules such as E-cadherin are responsible for discrimination of dermal and epidermal melanocytes in mouse (Kunisada et al., 2000; Nishimura et al., 1999). In human melanocytes, E-cadherin was indicated as a major mediator of their adhesion to skin keratinocytes (Tang et al., 1994). It could be that the forced expression of proper adhesion molecules such as those of the cadherin family might confer on the dermal melanocytes the ability to function as stem cells in the hair follicle.

It was reported that human mesenchymal cells co-cultured with epidermal keratinocyte differentiated into E-cadherin-expressing melanocytes at least in vitro (Li et al., 2010), suggesting a critical role of keratinocytes for melanocyte development. However, it should be noted that after the hair reconstitution assay with combinations containing only dermal melanocyte populations, we never observed the pigmented reconstituted hair. Considering that the hair reconstitution assay nearly recapitulates the entire developmental process, starting from the hair follicle from singly dissociated cells, dermal melanocytes could readily be associated with wild-type follicular keratinocytes during the regeneration process and directed to express proper cadherins necessary for their integration into regenerating hair follicles.

We induced dermal melanocytes in laboratory mice by the forced expression of ET3 or HGF, and this might have put the melanocytes in a highly non-physiological state. However, the characteristic phenotypes of *KitV620A* and *hk14-ET3* or *KitV620A* and *hk14-HGF* double transgenic mice resemble the skin phenotypes of polar bears, silky fowls or other animals with white coats but pigmented skin (Uehara et al., 2009). The fact that the expression of a single factor in the skin keratinocytes is enough to change the dermal or epidermal skin pigmentation through the control of the site-specific distribution of melanocytes is indicative of the close relationship between melanocytes and the adaptation strategy of animal coat color.

Our results suggest the possible early separation of melanocyte sub-lineages that migrate either into the epidermis or into the dermis, and these fundamental biological findings might provide important advances in the clinical treatment of diseases such as melanocytosis, vitiligo, and melanomas.

Methods

Animals

All animal experiments were approved by the Animal Research Committee of the Graduate School of Medicine, Gifu University. ICR mice, C57BL/6 mice, nude mice (*nu/nu*), and C3H mice were obtained from Japan SLC (Shizuoka, Japan). The following transgenic mice were maintained in our animal facility: those generated with the *human cytokeratin 14 promoter (hk14) driving ET3 cDNA*, referred to as *hk14-ET3* transgenic mice (Yamazaki et al., 2005); *Kit Val620Ala* transgenic mice (Tosaki et al., 2006); *DCT-lacZ* transgenic mice (Mackenzie et al., 1997); and C57BL/6 background *CAG-EGFP* mice (a gift from M. Okabe, Osaka University, Osaka, and RIKEN, BRC, Japan). *CAG-CAT-EGFP* mice (Kawamoto et al., 2000; a gift from J. Miyazaki, Osaka University, Osaka, Japan) were bred with $Dct^{tm1(Cre)Bee}$ mice (a gift from F. Beermann, Swiss Institute for Experimental Cancer Research, Epalinges, Switzerland) to generate compound heterozygotes (Osawa et al., 2005; Yonetani et al., 2008). Genotyping was performed as described previously (Guyonneau et al., 2004).

A *Dct-Venus* transgenic mouse line was generated by injecting a construct carrying a *Venus* gene (Nagai et al., 2002) under the control of *Dct* promoter (Mackenzie et al., 1997) into fertilized oocytes according to standard transgenic mouse procedures. The transgenic offspring were backcrossed with C57BL/6 mice for at least five generations.

Mice were housed in standard animal rooms with food and water provided ad libitum under controlled humidity and temperature (22 ± 2°C) conditions. The room was illuminated by fluorescent lights that were on from 8:00 to 20:00 hr.

Hair follicle reconstitution assay

The hair follicle reconstitution assay was performed as described previously (Kamimura et al., 1997; Kishimoto et al., 1999) with minor modifications. Briefly, the skin was freshly prepared from one or two newborn mouse pups [postnatal day (P) 0–2] for each graft and treated with 0.25% trypsin/1 mM EDTA overnight at 4°C. Then, the epidermis was peeled off the underlying dermis; and each separated layer was dissected into very small pieces. The epidermal cells (primary keratinocytes) were incubated with constant agitation in 0.025% trypsin/0.1 mM EDTA treatment at 4°C for 1 hr. These epidermal cells were then dissociated by gentle pipetting, and the cell suspensions were subsequently strained through a 100-μm-pore cell strainer (BD Falcon™, BD Biosciences, San Jose, CA, USA). These epidermal cells were combined with 2×10^6 dermal papilla cells that had been obtained by dissociation of dermis by constant agitation in 0.35% collagenase (Wako, Osaka, Japan) in DMEM (Gibco, Scotland, UK) at 37°C for 1 hr, and then the cell mixture was centrifuged and resuspended in 200 μl of serum containing medium. We transferred the combined cells to a grafting chamber, which was then implanted into the dorsal skin of nude mice (nu/nu) at 5–6 weeks of age. The chamber was removed after 7–10 days. Hair follicle formation and hair growth were monitored 3 weeks after grafting and weekly thereafter.

Cell preparation

The cell preparation procedure was performed as described previously (Aoki et al., 2009) with minor modifications. Briefly, P0 or adult mice were sacrificed by decapitation, and their eyes, harderian glands, and nose were quickly dissected on ice. The eyes were separated into cornea, lens, and neural retina; each was dissected into very small pieces (Aoki et al., 2008a). The harderian glands were also dissected into very small fragments. The nasal vibrissae were collected from the opposite side of the epidermis (vibrissae hair follicle) one by one, and dissected into very small fragments. Small pieces of all these tissues were treated overnight at 4°C with 0.25% trypsin/1 mM EDTA (Invitrogen), 0.1% collagenase 1 (Sigma-Aldrich, St Louis, MO, USA) and 1× dispase (Roche, Basel, Switzerland). The cells of these small pieces were dissociated by gentle pipetting, and the cell suspensions were then strained through 100-μm-pore the cell strainer.

Hair plucking

In accordance with the telogen-hair plucking method (Potten, 1970), we plucked hairs generated in the hair reconstitution assay 3–4 weeks after the cells had been transferred to the grafting chamber on the back skin of nude mouse. Hairs were plucked a second time almost 7–8 weeks after the cell transfer.

Patch assay

The patch assay was performed as described previously (Zheng et al., 2005) with minor modifications. Cells were prepared as described above and were assayed in male nude (nu/nu) mice at 7–9 weeks of age. For each intracutaneous injection, 2×10^6 dermal cells and 0.5×10^6 single epidermal cells were resuspended in 50–70 ml of DMEM-F12 medium (Invitrogen) and injected via a

25-gauge needle (Terumo, Tokyo, Japan) into the hypodermis of the nude mouse skin, forming a bleb.

LacZ staining

LacZ staining was performed as reported in detail previously (Yoshida et al., 1996b). In brief, skin samples were fixed for 30 min in 2% paraformaldehyde supplemented with 0.2% glutaraldehyde and 0.02% Tween 20. After three washes in phosphate-buffered saline (PBS), the samples were stained overnight at 37°C in 10 mM phosphate buffer (pH 7.2) containing 1.0 mM $MgCl_2$, 3.1 mM $K4[Fe(CN)_6]$, 3.1 mM $K3[Fe(CN)_6]$ and 2 mg/ml X-Gal. The staining reaction was stopped by washing in PBS. The specimens were post-fixed overnight in 10% formalin in phosphate buffer (pH 7.2).

Histology

Mice were killed with an overdose of sodium pentobarbital (200 mg/kg). Samples of skin were dissected and fixed by immersion overnight in 10% formalin in phosphate buffer (pH 7.2). The methods used for histological analysis were described in detail previously (Aoki et al., 2008c). Briefly, the skin samples were dehydrated with ethanol, soaked in xylene, and embedded in paraffin. Horizontal serial sections were prepared at a thickness of 3 μm, stained with hematoxylin and eosin (HE), and observed under an Olympus BX-60 microscope (Olympus, Tokyo, Japan). Images were captured with an Olympus DP70 digital camera.

Acknowledgements

We thank Dr. Jiro Kishimoto and Ritsuro Ideta for teaching the techniques of the hair reconstitution assay, Kyoko Takahashi for her excellent technical assistance, and Drs Tomohisa Hirobe and Hisahiro Yoshida for their thoughtful advice. We also thank Dr. J. Miyazaki for *CAG-CAT-GFP* mice, Dr. I. Jackson for *Dct-lacZ* mice, Dr. M. Okabe for *CAG-EGFP* mice, and Dr. F. Beermann for *Dct*$^{tm1(Cre)Bee}$ mice. This work was supported by grants from the Japan Society for the Promotion of Science and Research, a Fellowship from the Japan Society for the Promotion of Science for Young Scientists (H.A.), and a grant from the Ministry of Education, Science, Sports, and Culture of Japan.

References

Adameyko, I., Lallemend, F., Aquino, J.B. et al. (2009). Schwann cell precursors from nerve innervation are a cellular origin of melanocytes in skin. Cell *139*, 366–379.

Alexeev, V., and Yoon, K. (2006). Distinctive role of the cKit receptor tyrosine kinase signaling in mammalian melanocytes. J. Invest. Dermatol. *126*, 1102–1110.

Aoki, H., Yoshida, H., Hara, A., Suzuki, T., and Kunisada, T. (2008a). Transplantation of melanocytes into iris: method for iris repigmentation. Transplantation *85*, 492–494.

Aoki, H., Hara, A., Motohashi, T., Chem, H., and Kunisada, T. (2008b). Iris as a recipient tissue for pigment cells: organized in vivo differentiation of melanocytes and pigmented epithelium derived from embryonic stem cells in vitro. Dev. Dyn. *237*, 2394–2404.

Aoki, H., Hara, A., Niwa, M., Motohashi, T., Suzuki, T., and Kunisada, T. (2008c). Transplantation of cells from eye-like structures differentiated from embryonic stem cells in vitro and in vivo regeneration of retinal ganglion-like cells. Graefes Arch. Clin. Exp. Ophthalmol. *246*, 255–265.

Aoki, H., Yamada, Y., Hara, A., and Kunisada, T. (2009). Two distinct types of mouse melanocyte: differential signaling requirement for the maintenance of non-cutaneous and dermal versus epidermal melanocytes. Development *136*, 2511–2521.

Guyonneau, L., Murisier, F., Rossier, A., Moulin, A., and Beermann, F. (2004). Melanocytes and pigmentation are affected in dopachrome tautomerase knockout mice. Mol. Cell. Biol. *24*, 3396–3403.

Hall, B.K. (2009). The Neural Crest and Neural Crest Cells in Vertebrate Development and Evolution. (New York: Springer-Verlag).

Hirobe, T. (1984). Histochemical survey of the distribution of the epidermal melanoblasts and melanocytes in the mouse during fetal and postnatal periods. Anat Rec. *208*, 589–594.

Jackson, I.J. (1993). Molecular genetics. Colour-coded switches. Nature *362*, 587–588.

Jeon, S., Kim, N.H., Kim, J.Y., and Lee, A.Y. (2009). Stem cell factor induces ERM proteins phosphorylation through PI3K activation to mediate melanocyte proliferation and migration. Pigment Cell Melanoma Res. *22*, 77–85.

Kamimura, J., Lee, D., Baden, H.P., Brissette, J., and Dotto, G.P. (1997). Primary mouse keratinocyte cultures contain hair follicle progenitor cells with multiple differentiation potential. J. Invest. Dermatol. *109*, 534–540.

Kawamoto, S., Niwa, H., Tashiro, F., Sano, S., Kondoh, G., Takeda, J., Tabayashi, K., and Miyazaki, J. (2000). A novel reporter mouse strain that expresses enhanced green fluorescent protein upon Cre-mediated recombination. FEBS Lett. *470*, 263–268.

Kelsh, R.N., Harris, M.L., Colanesi, S., and Erickson, C.A. (2009). Stripes and belly-spots – a review of pigment cell morphogenesis in vertebrates. Semin. Cell Dev. Biol. *20*, 90–104.

Kishimoto, J., Ehama, R., Wu, L., Jiang, S., Jiang, N., and Burgeson, R.E. (1999). Selective activation of the versican promoter by epithelial-mesenchymal interactions during hair follicle development. Proc. Natl Acad. Sci. U S A *96*, 7336–7341.

Kopan, R., Lee, J., Lin, M.H., Syder, A.J., Kesterson, J., Crutchfield, N., Li, C.R., Wu, W., Books, J., and Gordon, J.I. (2002). Genetic mosaic analysis indicates that the bulb region of coat hair follicles contains a resident population of several active multipotent epithelial lineage progenitors. Dev. Biol. *242*, 44–57.

Kunisada, T., Yoshida, H., Yamazaki, H., Miyamoto, A., Hemmi, H., Nishimura, E., Shultz, L.D., Nishikawa, S., and Hayashi, S. (1998). Transgene expression of steel factor in the basal layer of epidermis promotes survival, proliferation, differentiation and migration of melanocyte precursors. Development *125*, 2915–2923.

Kunisada, T., Yamazaki, H., Hirobe, T., Kamei, S., Omoteno, M., Tagaya, H., Hemmi, H., Koshimizu, U., Nakamura, T., and Hayashi, S.I. (2000). Keratinocyte expression of transgenic hepatocyte growth factor affects melanocyte development, leading to dermal melanocytosis. Mech. Dev. *94*, 67–78.

Le Douarin, N.M., and Kalcheim, C. (1999). The Neural Crest, 2nd edn. (New York: Cambridge University Press).

Li, L., Fukunaga-Kalabis, M., Yu, H., Xu, X., Kong, J., Lee, J.T., and Herlyn, M. (2010). Human dermal stem cells differentiate into functional epidermal melanocytes. J. Cell Sci. *123*, 853–860.

Lichti, U., Weinberg, W.C., Goodman, L., Ledbetter, S., Dooley, T., Morgan, D., and Yuspa, S.H. (1993). In vivo regulation of murine hair growth: insights from grafting defined cell populations onto nude mice. J. Invest. Dermatol. *101*, 124S–129S.

Mackenzie, M.A., Jordan, S.A., Budd, P.S., and Jackson, I.J. (1997). Activation of the receptor tyrosine kinase Kit is required for the proliferation of melanoblasts in the mouse embryo. Dev. Biol. *192*, 99–107.

Mayer, T.C., and Fishbane, J.L. (1972). Mesoderm-ectoderm interaction in the production of the agouti pigmentation pattern in mice. Genetics *71*, 297–303.

Monroy, A., and Moscona, A.A. (1979). Introductory Concepts in Developmental Biology. (Chicago: University of Chicago Press).

Moscona, A. (1961). Rotation-mediated histogenetic aggregation of dissociated cells. A quantifiable approach to cell interactions in vitro. Exp. Cell Res. *22*, 455–475.

Nagai, T., Ibata, K., Park, E.S., Kubota, M., Mikoshiba, K., and Miyawaki, A. (2002). A variant of yellow fluorescent protein with fast and efficient maturation for cell-biological applications. Nat. Biotechnol. *20*, 87–90.

Nishimura, E.K., Yoshida, H., Kunisada, T., and Nishikawa, S.I. (1999). Regulation of E- and P-cadherin expression correlated with melanocyte migration and diversification. Dev. Biol. *215*, 155–166.

Nishimura, E.K., Jordan, S.A., Oshima, H., Yoshida, H., Osawa, M., Moriyama, M., Jackson, I.J., Barrandon, Y., Miyachi, Y., and Nishikawa, S. (2002). Dominant role of the niche in melanocyte stem-cell fate determination. Nature *416*, 854–860.

Ollmann, M.M., Wilson, B.D., Yang, Y.K., Kerns, J.A., Chen, Y., Gantz, I., and Barsh, G.S. (1997). Antagonism of central melanocortin receptors in vitro and in vivo by agouti-related protein. Science *278*, 135–138.

Osawa, M., Egawa, G., Mak, S.S., Moriyama, M., Freter, R., Yonetani, S., Beermann, F., and Nishikawa, S. (2005). Molecular characterization of melanocyte stem cells in their niche. Development *132*, 5589–5599.

Oshima, H., Rochat, A., Kedzia, C., Kobayashi, K., and Barrandon, Y. (2001). Morphogenesis and renewal of hair follicles from adult multipotent stem cells. Cell *104*, 233–245.

Potten, C.S. (1970). Radiation depigmentation of mouse hair: effect of the hair growth cycle on the sensitivity. J. Invest. Dermatol. *55*, 410–418.

Randall, V.A., Jenner, T.J., Hibberts, N.A., De Oliveira, I.O., and Vafaee, T. (2008). Stem cell factor/c-Kit signalling in normal and androgenetic alopecia hair follicles. J. Endocrinol. *197*, 11–23.

Tang, A., Eller, M.S., Hara, M., Yaar, M., Hirohashi, S., and Gilchrest, B.A. (1994). E-cadherin is the major mediator of human melanocyte adhesion to keratinocytes in vitro. J. Cell Sci. *107*, 983–992.

Tosaki, H., Kunisada, T., Motohashi, T., Aoki, H., Yoshida, H., and Kitajima, Y. (2006). Mice transgenic for Kit(V620A): recapitulation of piebaldism but not progressive depigmentation seen in humans with this mutation. J. Invest. Dermatol. *126*, 1111–1118.

Tsunenaga, M., and Ideta, R. (2002). Abstracts of the 16th Annual Meeting of the JSPCR, Nagoya, Japan. Pigment Cell Res. *15*, 472.

Uehara, S., Kawasaki, A., and Yamamoto, H. (2009). Classic versus non-classic: a survival Kit for life in the skin. Pigment Cell Melanoma Res. *22*, 706–708.

Wehrle-Haller, B., and Weston, J.A. (1997). Receptor tyrosine kinase-dependent neural crest migration in response to differentially localized growth factors. Bioessays *19*, 337–345.

Yajima, I., and Larue, L. (2008). The location of heart melanocytes is specified and the level of pigmentation in the heart may correlate with coat color. Pigment Cell Melanoma Res. *21*, 471–476.

Yamazaki, H., Sakata, E., Yamane, T., Yanagisawa, A., Abe, K., Yamamura, K., Hayashi, S., and Kunisada, T. (2005). Presence and distribution of neural crest-derived cells in the murine developing thymus and their potential for differentiation. Int. Immunol. *17*, 549–558.

Yonetani, S., Moriyama, M., Nishigori, C., Osawa, M., and Nishikawa, S. (2008). In vitro expansion of immature melanoblasts and their ability to repopulate melanocyte stem cells in the hair follicle. J. Invest. Dermatol. *128*, 408–420.

Yoshida, H., Kunisada, T., Kusakabe, M., Nishikawa, S., and Nishikawa, S.I. (1996a). Distinct stages of melanocyte differentiation revealed by anlaysis of nonuniform pigmentation patterns. Development *122*, 1207–1214.

Yoshida, H., Hayashi, S., Shultz, L.D., Yamamura, K., Nishikawa, S., Nishikawa, S., and Kunisada, T. (1996b). Neural and skin cell-specific expression pattern conferred by steel factor regulatory sequence in transgenic mice. Dev. Dyn. *207*, 222–232.

Zheng, Y., Du, X., Wang, W., Boucher, M., Parimoo, S., and Stenn, K. (2005). Organogenesis from dissociated cells: generation of mature cycling hair follicles from skin-derived cells. J. Invest. Dermatol. *124*, 867–876.

Supporting information

Additional Supporting Information may be found in the online version of this article:

Figure S1. Regenerated hairs before and after plucking.

Figure S2. Hairs reconstituted in the hair reconstitution assay.

Figure S3. Melanocyte localization in our transgenic mice.

Figure S4. Observation of the DCT-LacZ-positive unpigmented melanocytes.

Please note: Wiley-Blackwell are not responsible for the content or functionality of any supporting materials supplied by the authors. Any queries (other than missing material) should be directed to the corresponding author for the article.

The American Journal of Pathology, Vol. 178, No. 4, April 2011

DOI: 10.1016/j.ajpath.2011.01.004

Stem Cells, Tissue Engineering, and Hematopoetic Elements

Cytotoxic T Lymphocytes Efficiently Recognize Human Colon Cancer Stem-Like Cells

Satoko Inoda,*†‡ Yoshihiko Hirohashi,* Toshihiko Torigoe,* Rena Morita,* Akari Takahashi,* Hiroko Asanuma,§ Munehide Nakatsugawa,* Satoshi Nishizawa,* Yasuaki Tamura,* Tetsuhiro Tsuruma,† Takeshi Terui,‡ Toru Kondo,¶ Kunihiko Ishitani,‡ Tadashi Hasegawa,§ Koichi Hirata,† and Noriyuki Sato*

From the Department of Pathology, First Department of Surgery,† and Division of Clinical Pathology,‡ Sapporo Medical University School of Medicine, Sapporo; the Higashi Sapporo Hospital,‡ Sapporo; and the Team for Cell Lineage Modulation,¶ RIKEN Center for Developmental Biology, Kobe, Japan*

Cancer stem-like cells (CSCs) and tumor-initiating cells (TICs) are a small population of cancer cells that share three properties: tumor initiating ability, self-renewal, and differentiation. These properties suggest that CSCs/TICs are essential for tumor maintenance, recurrence, and distant metastasis. Here, we show that cytotoxic T lymphocytes (CTLs) specific for the tumor-associated antigen CEP55 can efficiently recognize colon CSCs/TICs both *in vitro* and *in vivo*. Using Hoechst 33342 dye staining, we isolated CSCs/TICs as side population (SP) cells from colon cancer cell lines SW480, HT29, and HCT15. The SP cells expressed high levels of the stem cell markers SOX2, POU5F1, LGR5, and ALDH1A1 and showed resistance to chemotherapeutic agents such as irinotecan or etoposide.To evaluate the susceptibility of SP cells to CTLs, we used CTL clone 41, which is specific for the CEP55-derived antigenic peptide Cep55/c10orf3_193 (10) (VYVKGLLAKI). The SP cells expressed HLA class I and CEP55 at the same level as the main population cells. The SP cells were susceptible to CTL clone 41 at the same level as main population cells. Furthermore, adoptive transfer of CTL clone 41 inhibited tumor growth of SW480 SP cells *in vivo*. These observations suggest that Cep55/c10orf3_193(10) peptide-based cancer vaccine therapy or adoptive cell transfer of the CTL clone is a possible approach for targeting chemotherapy-resistant colon CSCs/TICs. *(Am J Pathol 2011, 178:1805–1813; DOI: 10.1016/j.ajpath.2011.01.004)*

Colon cancer is one of the most common malignancies worldwide. With recent progress in treatment, the prognosis has improved to some extent. In advanced disease, however, the prognosis remains unfavorable, because of recurrence, distant metastasis, and resistance to treatment. Thus, novel treatment modalities are needed.

Cancers contain morphologically heterogeneous populations. This fact has led to the cancer stem cell theory,[1] the idea that cancers are composed of several types of cells, and that only a small population of cancer cells that can regenerate cancer tissues, much as normal tissue can be regenerated only by a small population of stem-like cells. Recently, cancer stem-like cells and tumor-initiating cells (CSCs/TICs) have been isolated from various types of malignancies, including colon cancer.[2–6] In colon cancer, CSCs/TICs can reinitiate tumors that resemble mother colon cancer tissues morphologically when transplanted into immunodeficient mice.[3] Furthermore, these CSCs/TICs have higher tumorigenic potential than do non-CSCs/TICs. Previous reports have shown that CSCs/TICs are resistant to a variety of treatments, including chemotherapy and radiotherapy, with varied mechanisms of resistance, including high expression of drug transporters, relative cell cycle quiescence, high levels of DNA repair machinery, and resistance to apoptosis.[7] These reports[3–6] support the hypothesis that malignant cancers comprise heterogeneous populations that organize in a hierarchical differentiation model. The CSCs/TICs are located at the top of this hierarchy, and targeting CSCs/TICs is essential to achieve efficient effects for treatment of malignant diseases. Recently, some trials targeting CSCs/TICs have been reported for hema-

Supported in part by a grant-in-aid for scientific research from the Ministry of Education, Culture, Sports, Science and Technology of Japan (N.S.) and by the Program for Developing the Supporting System for Upgrading Education and Research under the Ministry of Education, Culture, Sports, Science and Technology of Japan (N.S.).

Accepted for publication January 4, 2011.

CME Disclosure: None of the authors disclosed any relevant financial relationships.

Address reprint requests to Yoshihiko Hirohashi, M.D., Ph.D., Department of Pathology, Sapporo Medical University, School of Medicine, South-1 West-17, Chuo-ku, Sapporo 060-8556, Japan. E-mail: hirohash@sapmed.ac.jp.

topoietic malignancies.[8] Hedgehog signaling is essential for maintenance of myeloid leukemia stem cells, and inhibition of hedgehog signaling by cyclopamine is effective for imatinib-resistant myeloid leukemia.[9] To date, however, no such CSC/TIC targeting approach has been reported for colon cancer.

In the present study, we evaluated the efficiency of CTL-based immunotherapy targeting colon CSCs/TICs. Using Hoechst 33342 dye, we isolated colon CSCs/TICs as side population (SP) cells from six colon cancer cell lines. The SP cells derived from SW480, HT29, and HCT15 showed higher tumorigenicity than did main population (MP) cells. On the other hand, SP cells from KM12LM, Lovo, and Colo320 did not show any increase in tumorigenicity, compared with MP cells. This suggests that SW480, HT29, and HCT15 SP cells (but not KM12LM, Lovo, and Colo320 SP cells) were enriched with CSCs/TICs. In RT-PCR analysis the SW480, HT29, and HCT15 SP cells showed a stem cell-like gene expression signature, including SOX2, POU5F1, LGR5, and ALDH1A1. Furthermore, these SP cells also showed resistance to chemotherapeutic agents, including irinotecan and etoposide. These observations support the idea that these SP cells had stem cell-like features. To assess the immunogenicity of SP cells, we evaluated the expression of HLA class I and of CEP55, which is a tumor-rejection antigen of breast and colon cancer.[10,11] The SP cells expressed HLA class I (and also HLA-A24) at the same level as MP cells. The SP cells also expressed CEP55 messenger RNA (mRNA) at the same level as MP cells in RT-PCR. To confirm the susceptibility of SP cells to cytotoxic T lymphocytes (CTLs), we used CTL clone 41, which recognizes CEP55 in an HLA-A24-restricted manner.[10] CTL clone 41 killed SW480, HT29, and HCT15 SP cells at the same level as it killed MP cells and presorted cells. These observations suggest that colon CSCs/TICs are also sensitive to CTLs, as non-CSC/TIC populations are. Furthermore, adoptive transfer of CTL clone 41 inhibited the tumor growth of SW480 SP cells in immunodeficient mice. These observations suggest that CTL-based colon cancer immunotherapy is efficient for colon CSCs/TICs. To our knowledge, the present study provides the first direct evidence that colon CSCs/TICs are susceptible to CTLs and thus opens possibilities for future applications in immunotherapy using CSC/TIC-specific vaccines.

Materials and Methods

Cell Lines

Colon adenocarcinoma cell lines SW480 (HLA-A*0201/2402), HCT15 (HLA-A*0201/2402), HT29 (HLA-A1/24), Lovo, and Colo320 were kind gifts of Dr. K. Imai (Sapporo, Japan), and KM12LM was a kind gift of Dr. K. Itoh (Kurume, Japan). All cell lines except K562 were cultured in Dulbecco's modified Eagle's medium (Sigma-Aldrich, St. Louis, MO) supplemented with 10% fetal bovine serum (Invitrogen, Carlsbad, CA). K562 was cultured in RPMI-1640 (Sigma-Aldrich) supplemented with 10% fetal bovine serum. HCT15-B2M, a stable transfectant of HCT15 cells with B2M ($\beta 2$ microglobulin) cDNA, was cultured in Dulbecco's modified Eagle's medium supplemented with 10% fetal bovine serum and 10 μg/mL puromycin (Sigma-Aldrich).[11]

Side Population Analysis

Side population analysis was performed as described previously, with some modifications.[12] Trypsinized cultured cells were washed with PBS and were resuspended at 37°C in Dulbecco's modified Eagle's medium supplemented with 5% fetal bovine serum. After 10 minutes preincubation, the cells were labeled with Hoechst 33342 dye (Lonza, Walkersville, MD) for 90 minutes at concentrations of 3.75 μg/mL for Colo320, 5 μg/mL for SW480 and Lovo, 7.5 μg/mL for HT29 and KM12LM, and 10 μg/mL for HCT15, with or without verapamil (Sigma-Aldrich), which is an inhibitor of ABC transporters, at concentrations of 50 μmol/L for SW480, HCT15, and Colo320, 75 μmol/L for Lovo, and 100 μmol/L for HT29. Cells were counterstained with 1 μg/mL propidium iodide to label dead cells. Next, 1×10^6 viable cells were analyzed and sorted using a BD FACSAria II fluorescence-activated cell sorting system (BD Biosciences, Franklin Lakes, NJ). The Hoechst dye was excited at 355 nm, and its fluorescence was measured at two wavelengths using optical filters 405 DF20 [450/20 nm bandpass filter O (Hoechst Blue)] and 635LP [635 nm longpass edge filter (Hoechst Red)]. Propidium iodide labeling was measured through a 630/BP30 filter for discrimination of dead cells.

Xenograft Model

The SP cells, MP cells, and presorted cells from colon cancer cell lines were mixed 1:1 by volume with Matrigel (BD Biosciences) and were injected subcutaneously into the backs of female 4- to 8-week-old nonobese diabetic/severe combined immunodeficiency (NOD/SCID) mice. Tumor size in cubic millimeters was assessed weekly with calipers and was calculated as Tumor Size = (Longest Diameter $\times$ Shortest Diameter^2)/2.

RT-PCR Analysis of SP and MP Cells

RT-PCR analysis was performed as described previously.[10] Total RNAs were isolated from both SP cells and MP cells using an RNeasy mini kit (Qiagen, Valencia, CA) according to the manufacturer's protocol. Complementary DNA (cDNA) was synthesized from 2 μg of total RNA by reverse transcription using SuperScript III reverse transcriptase (Invitrogen). The PCR amplification was performed in 20 μL of PCR mixture containing 1 μL of cDNA mixture, 0.5 μL of Taq DNA polymerase (Qiagen) and 4 pmol of primers. The PCR mixture was initially incubated at 98°C for 2 minutes, followed by 30 cycles of denaturation at 98°C for 15 seconds, annealing at 60°C for 30 seconds, and extension at 72°C for 30 seconds. The following primer pairs were used for RT-PCR analysis (forward and reverse, respectively): 5′-CATGATG-

GAGACGGAGCTGA-3′ and 5′-ACCCCGCTCGCCATGC-TATT-3′ for SOX2, with an expected PCR product size of 410 bp; 5′-TGGAGAAGGAGAAGCTGGAGCAAAA-3′ and 5′-GGCAGATGGTCGTTTGGCTGAATA-3′ for POU5F1, with an expected PCR product size of 163 bp; 5′-CTCTT CCTCAAACCGTCTGC-3′ and 5′-GATCGGAGGCTA-AGCAACTG-3′ for LGR5, with an expected PCR product size of 181 bp; 5′-TGTTAGCTGATGCCGACTTG-3′ and 5′-TTCTTAGCCCGCTCAACACT-3′ for ALDH1A1, with an expected PCR product size of 154 bp; 5′-TGAGTTT-GCCATCACAGAGC-3′ and 5′-TTGCTTGCTGGTGCAT-TAAC-3′ for CEP55, with an expected PCR product size of 521 bp; and 5′-ACCACAGTCCATGCCATCAC-3′ and 5′-TCCACCACCCTGTTGCTGTA-3′ for glyceraldehyde-3-phosphate dehydrogenase (GAPDH), with an expected product size of 452 bp. GAPDH was used as an internal control.

Quantitative Real-Time PCR Analysis

Quantitative real-time PCR was performed using an ABI PRISM 7000 sequence detection system (Applied Biosystems, Foster City, CA) according to the manufacturer's protocol. Primers and probes were designed by the manufacturer (TaqMan gene expression assays; Applied Biosystems). Thermal cycling was performed using 40 cycles of 95°C for 15 seconds followed by 60°C for 1 minute. Each experiment was done in triplicate, with normalization to the *GAPDH* gene as an internal control.

Flow Cytometric Analysis and Monoclonal Antibodies

Cells were incubated with mouse monoclonal antibodies at saturation concentration for 30 minutes on ice, washed with PBS, and stained with a polyclonal goat anti-mouse antibody coupled with fluorescein isothiocyanate for 30 minutes. Samples were analyzed using a BD FACSCalibur flow cytometry system (Becton Dickinson, Mountain View, CA). Anti-pan HLA class I (W6/32) and anti-HLA-A24 monoclonal antibodies (C7709A2.6 hybridoma, a kind gift from Dr. P.G. Coulie, Brussels, Belgium) were prepared from hybridomas.

Survival Studies for Etoposide and Irinotecan

We isolated SP and MP cells of SW480 and HCT15 and seeded them into 96-well culture plates at 1×10^4 cells per well for each population of cells. The cells in both populations were treated with etoposide (1 and 5 μg/mL) or irinotecan (40 and 400 μg/mL for SW480, 10 and 100 μg/mL for HCT15). After 72 hours of exposure to the chemotherapeutic agents, viability of the cells was determined using the SOD assay kit WST-1, which was performed according to the manufacturer's protocol (Dojindo Molecular Technologies, Kumamoto, Japan; Rockville, MD).

Cytotoxicity Assay for SP Cells with CTL Clone 41

We had previously established CTL clone 41, which recognizes an HLA-A24 restricted antigenic peptide (VYVK-GLLAKI) termed Cep55/c10orf3_193(10), from an HLA-A24-positive breast cancer patient's peripheral blood mononuclear cells.[8] The lytic activity of CTL clone 41 for SP cells, MP cells, and presorted cells was evaluated by ^{51}Cr release assay. Briefly, SP cells, MP cells and presorted cells were labeled with 100 μCi of ^{51}Cr for 1 hour at 37°C, washed four times with PBS, and resuspended in AIM-V medium (Invitrogen). The ^{51}Cr-labeled target cells (2000 cells/well) were then incubated with various numbers of effector cells for 6 hours at 37°C in 96-well culture plates. Radioactivity of the culture supernatant was measured with a gamma counter. The percentage of cytotoxicity was calculated as follows: % Specific Lysis = (Experimental Release − Spontaneous Release) × 100/(Maximum Release − Spontaneous Release). Target cells were treated with 100 units/mL interferon-γ for 48 hours before the assay.

Winn Assay

SW480 SP cells were mixed with CTL clone 41 at a ratio of 1 SP cell to 10 CTL cells. The resulting mixture (200 μL with 1×10^6 CTL clone 41 and 1×10^5 SP cells) was injected subcutaneously into the backs of NOD/SCID mice. A control group of five mice was injected with SP cells alone. Tumor size was assessed weekly.

CTL Adoptive Transfer

NOD/SCID mice were inoculated subcutaneously on the back with 1×10^3 SW480 SP cells. Three weeks later, when the tumor started to be palpable, 5×10^4 Cep55/c10orf3_193(10)-specific CTL clone cells or PBS was injected intravenously. The same adoptive transfer procedure was performed 4 weeks after inoculation with SP cells. Tumor size was assessed weekly.

Statistical Analysis

In the xenograft model, survival studies using chemotherapeutic agents, cytotoxicity assay, Winn assay, and adoptive transfer model, the data were analyzed using the Mann-Whitney *U*-test, with $P < 0.05$ conferring statistical significance.

Results

Isolation of Colon CSCs/TICs as SP Cells

Several methods to isolate colon cancer CSCs/TICs has been reported, including cell surface markers such as CD44 or PROM1 (CD133), SP cells, and the Aldefluor assay.[3–6,13] In the present study, we isolated colon CSCs/TICs using SP cell analysis. Several colon cancer cell lines were dyed with Hoechst 33342 and then analyzed with a BD FACSAria II flow cytometer as